ResearchGate

See discussions, stats, and author profiles for this publication at: https://www.researchgate.net/publication/331941961

Modeling and Analysis of Multi-Purpose Hybrid Surgical Robot

Conference Paper · January 2019

DOI: 10.1109/IBCAST.2019.8667161

CITATIONS
0

READS
120

3 authors, including:

Haroon Khan
Oslo Metropolitan University
18 PUBLICATIONS **141** CITATIONS
SEE PROFILE

Zareena Kausar
Khwaja Fareed University of Engineering & Information Technology
53 PUBLICATIONS **281** CITATIONS
SEE PROFILE

All content following this page was uploaded by Haroon Khan on 25 June 2020.

The user has requested enhancement of the downloaded file.

Modeling and Analysis of Multi-Purpose Hybrid Surgical Robot

1st Haroon Khan
Dept. of Mechatronics Engineering
Air University
Islamabad, Pakistan
*engrharoon1991@gmail.com

2nd Zareena Kausar
Dept. of Mechatronics Engineering
Air University
Islamabad, Pakistan
zareena.kausar@mail.au.edu.pk

3rd Salman Bari
Dept. of Mechatronics Engineering
Air University
Islamabad, Pakistan
salmanbari03@gmail.com

***Abstract*—Robotic surgery revolution has not just assisted surgeons to perform complicated surgeries but also increased accuracy, reduced risk, operative and recovery time. Parallel architecture is widely used for designing of surgical robots due to its advantage of low inertia and high precision. But their workspace is confined and limited to specific surgical procedures. In this research work, a hybrid architecture is proposed and its modeling and analysis is presented. This architecture includes both parallel and serial manipulators with six and two degree of freedom respectively. Kinematic analysis of hybrid platform is presented focusing on derivation of inverse kinematics for the surgical tool positioning. Dynamic modelling of hybrid surgical robot is performed in MATLAB Simscape Multibody for analysis and simulation. The positional accuracy of surgical system is achieved using feedback control. Design of hybrid surgical robot shows that the proposed system achieved better positional accuracy and desired workspace. Analysis of torque requirements in dynamic simulation shows that it is achievable for the desired hybrid surgical system.**

***Index Terms*—Surgical Robot, Hybrid Architecture, Kinematic modeling**

I. Introduction

Surgical robots have made considerable advancements in medical field which increases the accuracy of surgeries, reduce the time of surgery and also reduce the recovery time of the patient. On basis of kinematic structure, surgical robots are classified into three architectures namely serial architecture, parallel architecture and hybrid architecture [1]. Serial robots are most commonly used in industry due its main advantage of large workspace. But due to open kinematic chain and more weight (inertia) it is not reliable to use in high stiffness and accurate applications. Parallel robots are widely used in medical applications due to high stiffness and accuracy [2]. 1n 1985, PUMA 560 was used for first time in human brain biopsy. In 1998, ROBODOC™ 5 axis SCARA robot which consist of 2 revolute joint axes. It received Food and Drug Administration (FDA) clearance for total hip replacement [3], [4]. In [5], a new surgical serial design is proposed with consideration of required workspace with constrained outlined. Among serial surgical robots most popular serial robot for laparoscopic surgeries is Da Vinci which cleared FDA clearance in year 2000 for general laparoscopic surgeries [6]. In 2003, a major advancement came in spinal robotic surgery when a team of Israeli researcher presented the MiniAture Robot for Surgical (MARS) procedures [7]. MARS is based on six degree of freedom (DOF) parallel manipulator with work-volume and size of 10 cm^3 and 557 cm^3 respectively. The significance of MARS robot is its light weight (200g) which simplifies the registration process. The robot is used for pedical screw in spinal fusion and distal locking in intramedullary nailing [8], [9]. MARS progressed into SpineAssist and then to Renaissance which is now commercialized by Mazor Robotics (Cesarea, Israel). Kobler et al. developed a head mounted parallel kinematic robot for skull surgery. The robot design is based on Stewart-Gough platform. The base of platform is equipped with spherical heads which are implanted in patient skull [10]. The surgical tool is mounted on the moving platform which allows for guided intervention between the bone anchors e.g drilling access to cochlea, insertion of needle etc [10]. In orthopedics, for long bone deformity correction 6-DOF external fixator based on stewart platform is used. Later on, many different design were proposed and its development is still going on [11]. In [12], a computer assisted external fixator adjustable in all 6-DOf is developed. The fixator consists of two ring each ring has 3 pair of ball and joint. In [13], 6-DOF parallel robot with six linear actuators using ball and screw mechanism is proposed for cervical disc. A.Wolf et. al. [14] designed miniature bone-attached robotic system (MBARS) for jointed arthoplasty. The robot is based on Stewart platform with centralized tool at the center of top plate for bone grinding. In [15], another system for joint arhtoplasty named as hyBAR (Hybrid bone attached robot) is presented. The robot is based on serial-parallel structure with three DOF. In [16] describe two-armed micro-surgical robot for orbital manipulation and intraocular dexterity. For ease of ophthalmic microsurgical procedure 16 DOF robot is proposed. The frame of the robot is fixed to the patient head using bite plate without trauma to patient head. The two-identical robotic arm is composed of 6 DOF parallel robot and 2 DOF of IODR (Intra-Ocular Dexterity Robot). The 6 DOF parallel mechanism provides global precise positioning of eye and surgical tool inside the eye while the IODR provides intra-ocular dexterity. In this research multipurpose Hybrid Surgical Robot (HSR) is proposed with hypothesis that it will

978-1-5386-7729-2/19/$31.00©2019 IEEE

not only enhance workspace but give economical DOF which can be utilized in different type of surgical operations. Paper is organised as follow: conceptual design of the proposed surgical robot is presented in section II while kinematics model is laid in section III. Simulation Setup, results,conclusion and recommendations are presented in section IV,V and VI respectively.

II. Conceptual Design of Hybrid Surgical Robot

Conceptual design of HSR is developed using SOLIDWORKS. The parallel platform (PP) is basically Stewart-Platform and serial mechanism (SM) at top platform of PP with total 8 DOF as shown in Fig. 1. The size ratio between top and base plate is 2:3 to give static stability. Since different materials are studied the weight of robot with different material is shown in Table I. The total size of the robot is $5 \times 7 \times 7.4\ cm^3$

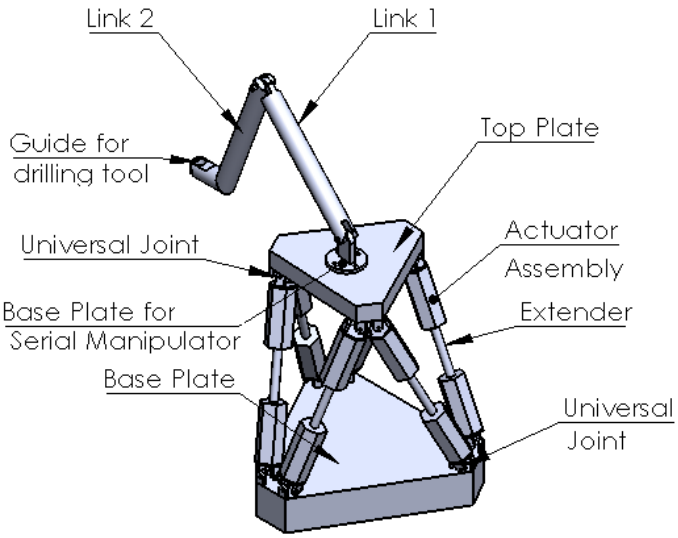

Fig. 1. SOLIDWORKS Model of the proposed HSR

TABLE I
WEIGHT OF HSR WITH DIFFERENT MATERIAL SELECTION

Sr. No.	Material	Weight (g)
1	Stainless Steel	245
2	Titanium	140
3	High Density Steel	30

III. Kinematic Modeling of HSR

Inverse kinematics gives joint parameters by providing desired position of end effector. Inverse kinematics for both the platforms are considered individually. The forward kinematics analysis is not recommended for this study because solution becomes complicated due to higher order non-linear equations [17].

A. Inverse Kinematics of the Parallel Platform

The set of actuation lengths required for linear actuator to reach the desired position and orientation are computed [18]. The frame assignment is shown in Fig. 3. The position and orientation of frame T is represented with (P_x, P_y, P_z) and (α, β, Γ). Points Bi and Ti are the connecting points while R_b

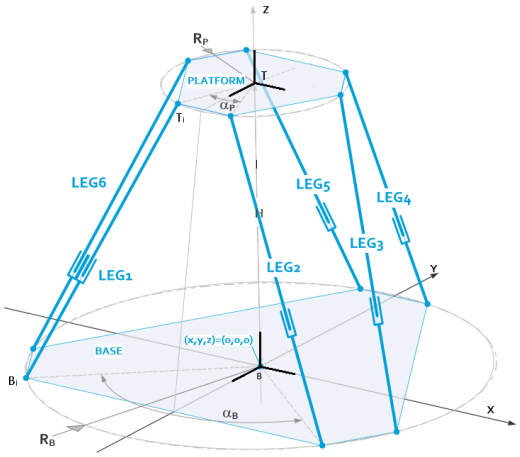

Fig. 2. Parallel platform schematic diagram

and R_p are radius of base and top platform respectively. Also, the separation angles between alternate points of base and top platform are denoted by α_B and α_p respectively. Points (Bi and Ti) can be determined by using (1) and (2).

$$T_i = \begin{bmatrix} T_{xi} \\ T_{yi} \\ T_{zi} \end{bmatrix} = \begin{bmatrix} R_p \cos(\lambda_j) \\ R_p \sin(\lambda_j) \\ 0 \end{bmatrix} \tag{1}$$

$$B_i = \begin{bmatrix} B_{xi} \\ B_{yi} \\ B_{zi} \end{bmatrix} = \begin{bmatrix} R_b \cos(\vartheta_i) \\ R_b \sin(\vartheta_i) \\ 0 \end{bmatrix} \tag{2}$$

$\vartheta_i = \vartheta_{i-1} + \alpha_B$, $\vartheta_i = \frac{i*180}{3} - \frac{\alpha_B}{2}$ for i=2,4,6
$\lambda_j = \frac{i*180}{3} - \frac{\alpha_P}{2}$, $\lambda_j = \lambda_{j-1} + \alpha_P$ for j=2,4,6

The values of α_B, α_p, R_b and R_p are respectively 106.36, 13.64, 29.463 mm and 19.31 mm. P and ${}^B R_T$ denotes position and rotation of the moving platform respectively. It can be represented by (3).

$${}^B R_T = R_z(\gamma) R_y(\beta) R_x(\alpha) = \begin{pmatrix} r_{11} & r_{12} & r_{13} \\ r_{21} & r_{22} & r_{23} \\ r_{31} & r_{32} & r_{33} \end{pmatrix} \tag{3a}$$

$${}^B R_T = \begin{pmatrix} C_\beta C_\gamma & C_\gamma S_\beta S_\gamma - S_\gamma C_\gamma & C_\alpha S_\beta S_\gamma + S_\alpha S_\gamma \\ C_\beta S_\gamma & S_\alpha S_\beta S_\gamma + C_\alpha C_\gamma & S_\alpha S_\beta C_\gamma - C_\alpha S_\gamma \\ -S_\beta & C_\beta S_\gamma & C_\beta C_\gamma \end{pmatrix} \tag{3b}$$

$$S_i = sin(i), C_i = cos(i), i = \alpha, \beta, \gamma \tag{3c}$$

The vector Li represent the length of ith leg can be written as:

$$L_i = R_{XYZ} T_i + P - B_i \tag{4}$$

$$P = \begin{bmatrix} P_x & P_y & P_z \end{bmatrix}^T \tag{5}$$

$$X_P^B = [P_x, P_y, P_z, \alpha, \beta, \gamma] \tag{6}$$

Knowing the vector X_P^B the length L_i of each leg of PP can be computed using (7).

$$\begin{aligned} L_i^2 = (P_x - B_{xi} - T_{xi}r_{11} + T_{yi}r_{12})^2 + (P_y - B_{yi} \\ + T_{xi}r_{21} + T_{yi}r_{22})^2 + (P_z + T_{xi}r_{31} + T_{yi}r_{32})^2 \end{aligned} \tag{7}$$

Where i = 1,2,3,4,5,6

B. Inverse Kinematics of the 2-link Serial Manipulator

The base of two link serial manipulator is connected at top plate center. Frames assigned to base joint and end-effector are (X_1,Y_1,Z_1) and $T_t = [X_t, Y_t, Z_t, \alpha_t, \beta_t, \gamma_t]$ respectively as shown in Fig.3. The joint angles can be calculated using

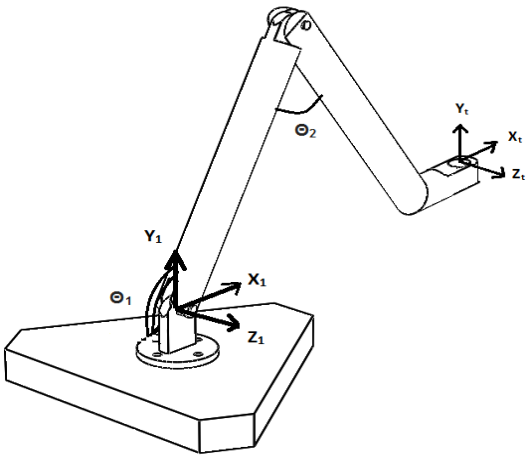

Fig. 3. Two link manipulator diagram

(8) and (9) [19].

$$\theta_2 = \arctan 2\,(s_2, c_2) \tag{8a}$$

$$c_2 = \frac{x_t^2 + y_t^2 - l_1^2 - l_2^2}{2 l_1 l_2} \tag{8b}$$

$$s_2 = \pm\sqrt{1 - c_2^2} \tag{8c}$$

$$\theta_1 = \arctan 2\,(y_t, x_t) - \arctan 2\,(k_2, k_1) \tag{9a}$$

$$k_1 = l_1 + l_2 c_2 \tag{9b}$$

$$k_2 = l_2 s_2 \tag{9c}$$

$$c_i = cos(\theta_i) \tag{9d}$$

$$s_i = sin(\theta_i) \tag{9e}$$

For i = 1,2. Where as l_1 and l_2 are the link lengths of serial manipulator.

C. Simulation Setup

To avoid complexity in simulating model dynamics and coupled ODEs, the HSR is modeled in SOLIDWORKS and then imported to Simscape Multibody. Simulation of Simscape Multibody is show in Fig.4. Simscape Multibody model contain all the required blocks such as trajectory generation block, controller block and other system blocks. Trajectory generating block generates required joint actuation and velocities provided to joint actuators to reach desired point.

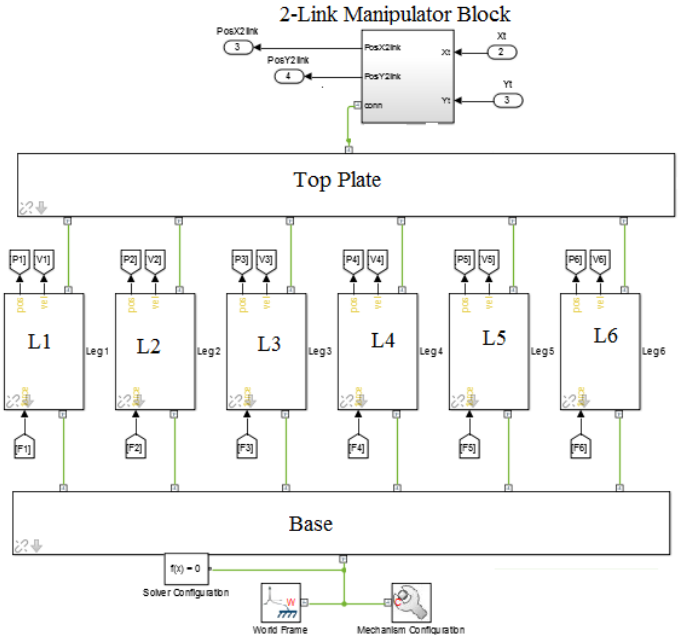

Fig. 4. Simscape Multibody model of the HSR of the HSR

IV. Results

Position plots, force and torque required to achieve the desired trajectory is discussed in this section in detail.

A. Position Plots

The simulate behavior of HSR set point are given to both the platforms. Global reference is assigned to baseplate of PP and both trajectories of platforms are observed with respect to it. We have set random set points as (5,5,50) and (-25,20) in millimeters for parallel platform and serial manipulator respectively. PID control is applied to regulate the manipulator to reach the set points. Results of X,Y and Z coordinates of PP are shown from Fig. 5 to Fig.7 and position plots of serial manipulator is shown in Fig.9 respectively. In Fig.5 to 7 initial overshoot in the results show that the system aggressively tends to achieve the desired position. The PID control however brings the platform back to the desired position. The response seems slightly sluggish but to achieve the accuracy required, the movement must be slow. If we examine the errors in plot shown in Fig.8 we can see that the error bound after the settling of the response is very low. the error eventually ends up fluctuating around zero but this fluctuation is in order

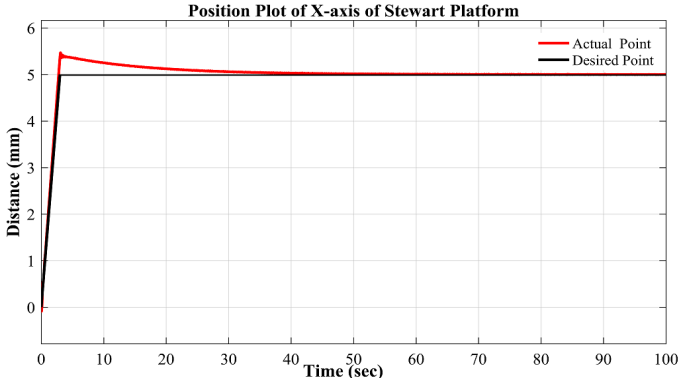

Fig. 5. Position plot of X-axis of parallel platform

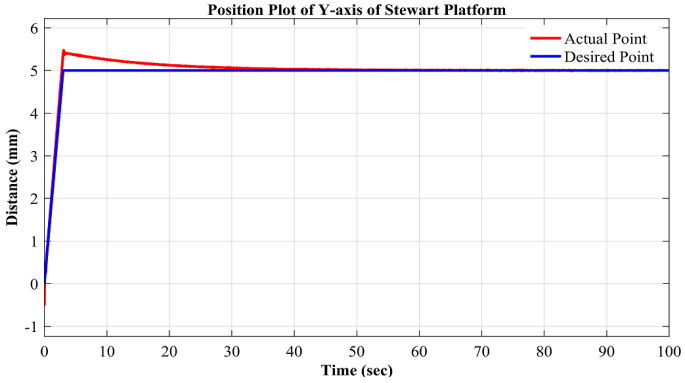

Fig. 6. Position plot of Y-axis of parallel platform

of microns. The plot for the position coordinates (x,y) for given point (-25,20) is shown in Fig.9. They show that 2 link manipulator attains the desired value in less than 10 secs. The error plots for x and y coordinate in Fig.10 which show that error also reaches zero values in the same amount of time. The value for X-axis and Y-axis still fluctuate in range of 3 to 4 millimeter and micrometers respectively. The above results conclude that both the platform able to attain the desired position in good time and with reasonable accuracy. Summary of errors in all the axis of HSR is shown in Table II.

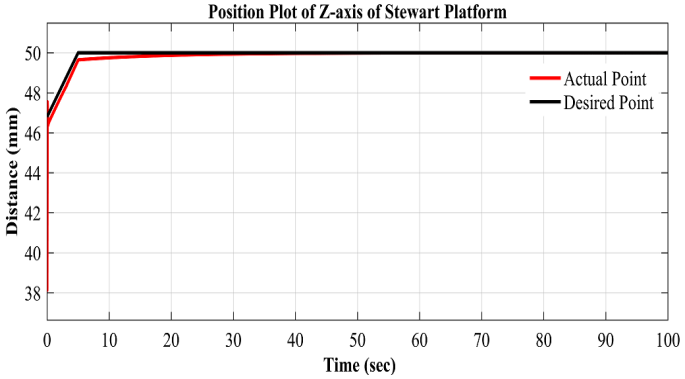

Fig. 7. Position plot of Z-axis of parallel platform

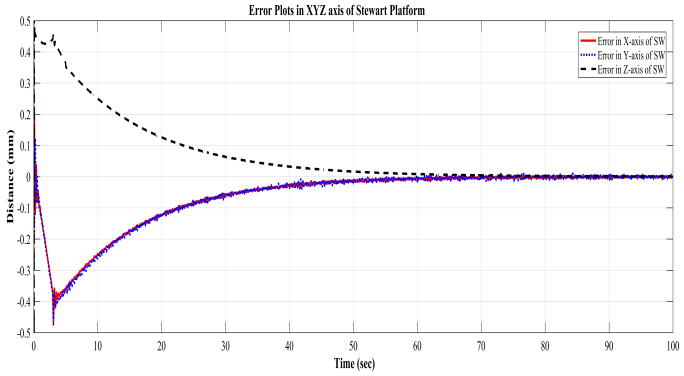

Fig. 8. Error plot of XYZ-axis of parallel platform

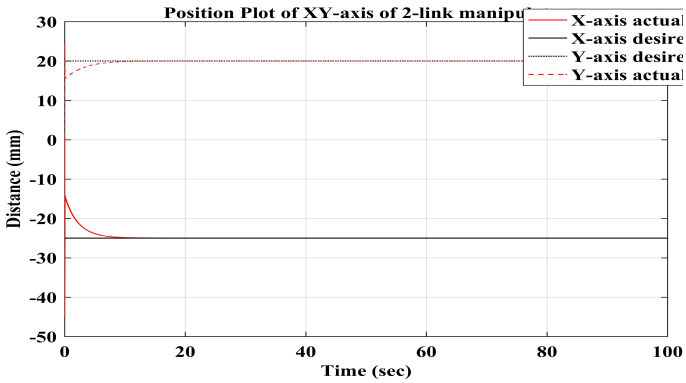

Fig. 9. Position plot of XY-axis of 2 link manipulator

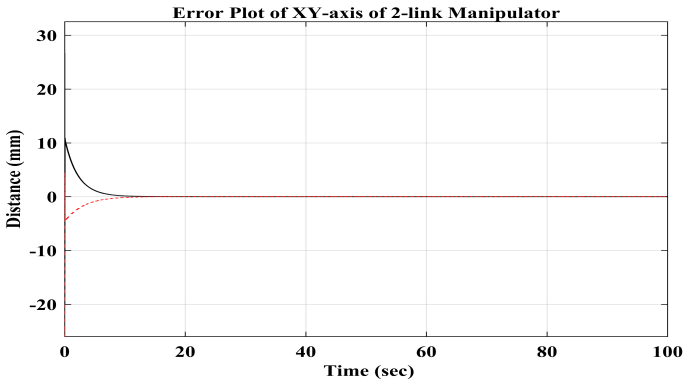

Fig. 10. Error plot of XY-axis of 2 link manipulator

TABLE II
SUMMERY OF ERROR IN POSITION PLOT

Sr.No	Platform	Axis	Error(mm)
1	Parallel Platform	X-axis	0.003
2	Parallel Platform	Y-axis	0.006
3	Parallel Platform	Z-axis	0.0010
4	Serial Manipulator	X-axis	0.004
5	Serial Manipulator	Y-axis	0.03

B. Force and Torque Requirements

Torques and force requirements acquired form joint sensors and actuators to reach the set points while simulating dynamic model of HSR in Simscape Multibody as shown in Fig.11 is discussed here. Force applied by each six linear actuators

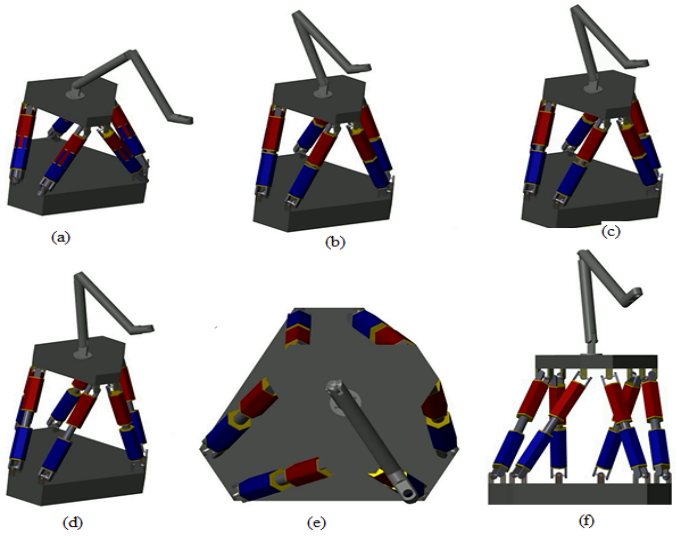

Fig. 11. Dynamic simulation of HSR (a) Initial Stage (b) Start reaching the desired point (DP) (c)Approaching DP (d) Reaching desired point(e) Top view of HSR after reaching (DP) (f) Side view of HSR after reaching DP

while simulating the HSR to reach the set point is shown from Fig.12 to Fig.17. As we can see that value of force start from zero and then for about first four seconds its values instantly increase as it tries to reach quickly. After then it settles down to quantify value. But as our HSR dose not settle to set value and still there is some error and controller is constantly putting an effort to keep the system closer to the set value. Due to which observe that force value fluctuates within a bounded region. These oscillation may arise from various sources. One of them could be that the control law is not efficient for full control of the system. The torque requirement for joint

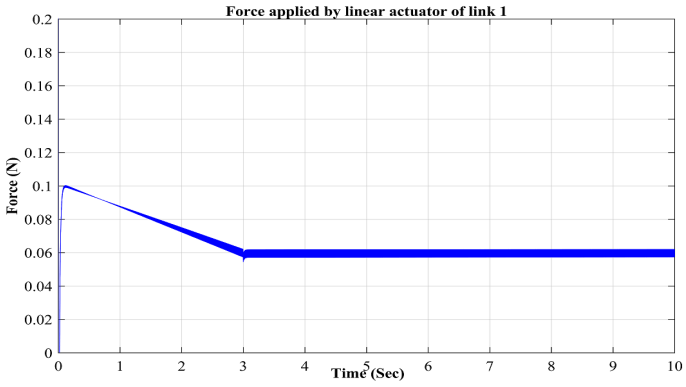

Fig. 12. Force applied by linear actuator of link 1

actuators of serial manipulator is shown in Fig.19 and Fig.18. Initially, the torque requirements for joint actuators in much

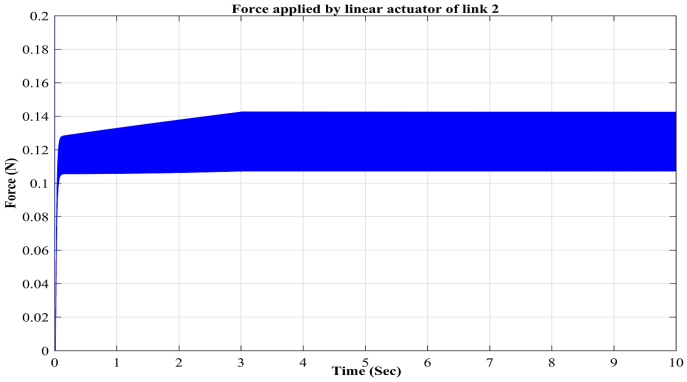

Fig. 13. Force applied by linear actuator of link 2

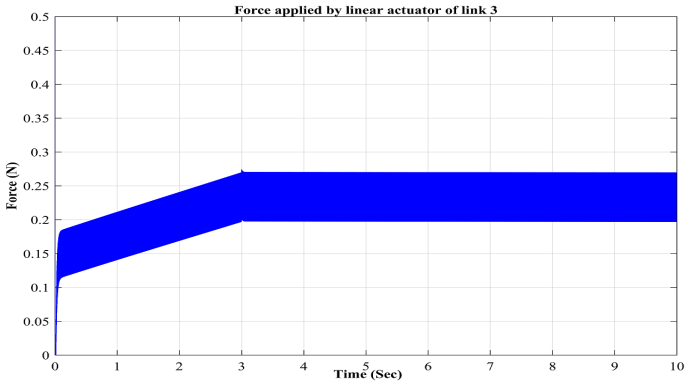

Fig. 14. Force applied by linear actuator of link 3

higher as its earlier discussed that it tries to reach the set value quickly. When the required position is achieved, torque applied is limited to certain bounded value as 0.06 Nm and 0.1 Nm for link 1 and 2 respectively. Torque does not become zero as for the position control, a continuous effort is being applied to keep the end effector close to the set position. One of the major effects of this fluctuations are the non-linearity in the system and also system does not settle to set value. Dynamic analysis results are summarized in TableIII.

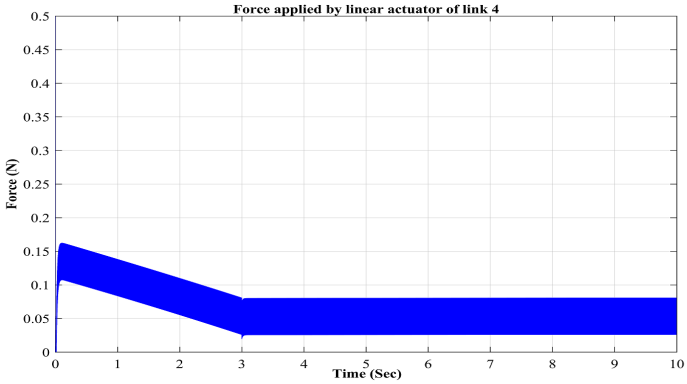

Fig. 15. Force applied by linear actuator of link 4

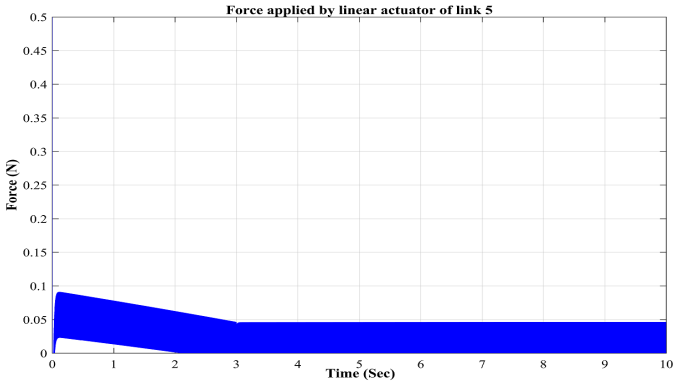

Fig. 16. Force applied by linear actuator of link 5

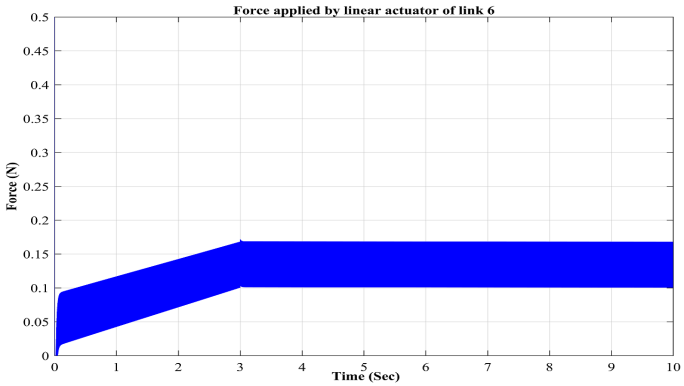

Fig. 17. Force applied by linear actuator of link 6

V. Conclusion and Recommendation

A conceptual design, kinematic and dynamic model of proposed hybrid surgical robot (HSR) is presented in this paper. Inverse kinematics of positing platform is performed to calculate required actuator lengths for PP and joints actuation of serial manipulator to reach the set point. A dynamic model was developed in MATLAB Simscape Multibody to calculate the required force and torques for linear and joint actuator to check the system requirements. Dynamic simulation results show that system force and torque requirements are achievable.

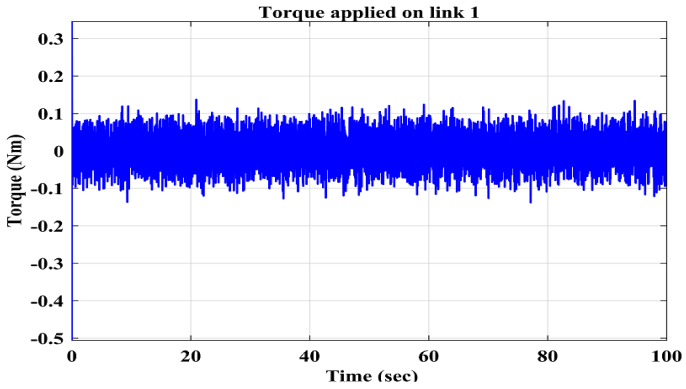

Fig. 18. Torque applied by link 1

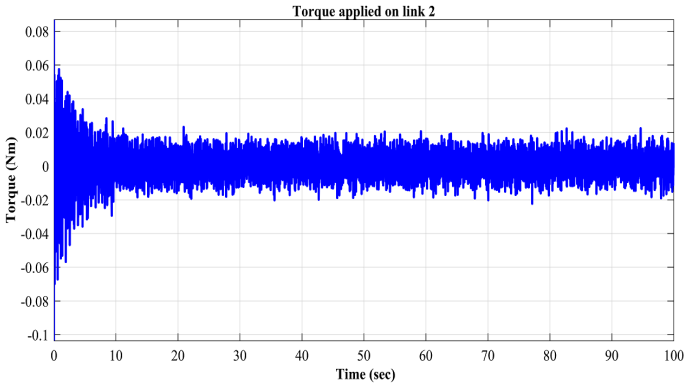

Fig. 19. Torque applied by link 2

TABLE III
Summery of force and torque requirement for HSR

Sr.No	Platform	Actuator /Joint	Force (N)	Torque (Nm)
1	Parallel Platform	Linear Actuator 1	0.06	-
2	Parallel Platform	Linear Actuator 2	0.14	-
3	Parallel Platform	Linear Actuator 3	0.26	-
4	Parallel Platform	Linear Actuator 4	0.04	-
5	Parallel Platform	Linear Actuator 5	0.05	-
6	parallel Platform	Linear Actuator 6	0.15	-
7	Serial Manipulator	Joint 1	-	0.1
8	Serial Manipulator	Joint 2	-	0.02

PID controller is implemented to control each actuator individually .Although PID controller tracks the HSR to desired accuracy of 1mm but still there is large room to test improve control law. Since both serial and parallel mechanisms are coupled, coupled non-linear ordinary differential equation may be developed for better control and understanding of system. Coupled dynamics equations can help to identify the effect of vibrations produced.

References

[1] N. Simaan, "Analysis and synthesis of parallel robots for medical applications," Ph.D. dissertation, Technion-Israel Institute of Technology, Faculty of Mechanical Engineering, 1999.

[2] Z. Pandilov and V. Dukovski, "Comparison of the characteristics between serial and parallel robots," *Acta Technica Corviniensis-Bulletin of Engineering*, vol. 7, no. 1, p. 143, 2014.

[3] P. Kazanzides, J. Zuhars, B. Mittelstadt, B. Williamson, P. Cain, F. Smith, L. Rose, and B. Musits, "Architecture of a surgical robot," in *Systems, Man and Cybernetics, 1992., IEEE International Conference on*. IEEE, 1992, pp. 1624–1629.

[4] A. P. Schulz, K. Seide, C. Queitsch, A. Von Haugwitz, J. Meiners, B. Kienast, M. Tarabolsi, M. Kammal, and C. Jürgens, "Results of total hip replacement using the robodoc surgical assistant system: clinical outcome and evaluation of complications for 97 procedures," *The International Journal of Medical Robotics and Computer Assisted Surgery*, vol. 3, no. 4, pp. 301–306, 2007.

[5] M. A. Laribi, M. Arsicault, T. Riviere, and S. Zeghloul, "Toward new minimally invasive surgical robotic system," in *Industrial Technology (ICIT), 2012 IEEE International Conference on*. IEEE, 2012, pp. 504–509.
[6] C.-H. Kuo and J. S. Dai, "Robotics for minimally invasive surgery: a historical review from the perspective of kinematics," in *International symposium on history of machines and mechanisms*. Springer, 2009, pp. 337–354.
[7] M. Shoham, M. Burman, E. Zehavi, L. Joskowicz, E. Batkilin, and Y. Kunicher, "Bone-mounted miniature robot for surgical procedures: Concept and clinical applications," *IEEE Transactions on Robotics and Automation*, vol. 19, no. 5, pp. 893–901, 2003.
[8] Z. Yaniv and L. Joskowicz, "Precise robot-assisted guide positioning for distal locking of intramedullary nails," *IEEE transactions on medical imaging*, vol. 24, no. 5, pp. 624–635, 2005.
[9] ——, "Robot-assisted distal locking of long bone intramedullary nails: Localization, registration, and in vitro experiments," in *International Conference on Medical Image Computing and Computer-Assisted Intervention*. Springer, 2004, pp. 58–65.
[10] J.-P. Kobler, J. Kotlarski, J. Öltjen, S. Baron, and T. Ortmaier, "Design and analysis of a head-mounted parallel kinematic device for skull surgery," *International journal of computer assisted radiology and surgery*, vol. 7, no. 1, pp. 137–149, 2012.
[11] D. Paley, "History and science behind the six-axis correction external fixation devices in orthopaedic surgery," *Operative techniques in orthopaedics*, vol. 21, no. 2, pp. 125–128, 2011.
[12] K. Seide, M. Faschingbauer, M. Wenzl, N. Weinrich, and C. Juergens, "A hexapod robot external fixator for computer assisted fracture reduction and deformity correction," *The International Journal of Medical Robotics and Computer Assisted Surgery*, vol. 1, no. 1, pp. 64–69, 2004.
[13] H. Tian, C. Wang, X. Dang, and L. Sun, "A 6-dof parallel bone-grinding robot for cervical disc replacement surgery," *Medical & biological engineering & computing*, vol. 55, no. 12, pp. 2107–2121, 2017.
[14] A. Wolf, B. Jaramaz, B. Lisien, and A. DiGioia, "Mbars: mini bone-attached robotic system for joint arthroplasty," *The International Journal of Medical Robotics and Computer Assisted Surgery*, vol. 1, no. 2, pp. 101–121, 2005.
[15] S. Song, A. Mor, and B. Jaramaz, "Hybar: hybrid bone-attached robot for joint arthroplasty," *The International Journal of Medical Robotics and Computer Assisted Surgery*, vol. 5, no. 2, pp. 223–231, 2009.
[16] W. Wei, R. Goldman, N. Simaan, H. Fine, and S. Chang, "Design and theoretical evaluation of micro-surgical manipulators for orbital manipulation and intraocular dexterity," in *Robotics and Automation, 2007 IEEE International Conference on*. IEEE, 2007, pp. 3389–3395.
[17] D. Jakobović and L. Budin, "Forward kinematics of a stewart platform mechanism," *Faculty of Electrical Engineering and Computing Faculty of Electrical Engineering and Computing Unska*, vol. 3, p. 10000, 2002.
[18] K. Liu, F. Lewis, G. Lebret, and D. Taylor, "The singularities and dynamics of a stewart platform manipulator," *Journal of Intelligent and Robotic Systems*, vol. 8, no. 3, pp. 287–308, 1993.
[19] J. J. Craig, *Introduction to robotics: mechanics and control*. Pearson/Prentice Hall Upper Saddle River, NJ, USA:, 2005, vol. 3.

View publication stats